Clays and Clay Minerals, Vol. 46, No. 4, 369–378, 1998.

IRON OXIDES IN A SOIL DEVELOPED FROM BASALT

A. T. GOULART,[1,2] J. D. FABRIS,[1] M. F. DE JESUS FILHO,[1,†] J. M. D. COEY,[3] G. M. DA COSTA[4] AND E. DE GRAVE[5‡]

[1] Departamento de Química, UFMG-Pampulha, 31270-901 Belo Horizonte, MG, Brazil

[2] On leave from Departamento de Química, UFV, 36571-000 Viçosa, MG, Brazil

[3] Department of Pure and Applied Physics, Trinity College, University of Dublin, Dublin 2, Ireland

[4] Departamento de Química, UFOP, 35400-000 Ouro Preto, MG, Brazil

[5] Department of Subatomic and Radiation Physics, University of Gent, B-9000 Gent, Belgium

Abstract—A dusky red Oxisol forming on a tholeiitic basalt is found to contain varying proportion of aluminous hematite (Hm) and titanoaluminous maghemite (Mh) in the different size fractions. Maghemite is the main iron oxide in the sand and silt fractions whereas Hm is dominant in the clay fraction, together with gibbsite (Gb), kaolinite (Ka), rutile (Rt) (and probably anatase, An) and Mh. Maghemite is also the major oxide mineral in the magnetic separates of soil fractions (sand, about 65% of the relative Mössbauer spectral area; silt, 60%). Hematite (sand, 30%; silt, 15%) and ilmenite (Im) (sand, 5%; silt, 16%) are also significantly present in the magnetic extract. Accessory minerals are Rt and An. No magnetite (Mt) was detected in any soil fraction. Sand- and silt-size Mh have similar nature (a_0 = 0.8319 ± 0.0005 nm; about 8 mol% of Al substitution; saturation magnetization of 49 J T^{-1} kg^{-1}), and certainly a common origin. Lattice parameters of clay-Mh are more difficult to deduce, as magnetic separation was ineffective in removing nonmagnetic phases. Al content in Hm varies from 14 mol% (clay and silt) to 20 mol% (sand). The proposed cation distribution on the spinel sites of the sand-size Mh is:

$$[Fe_{0.92}Al_{0.08}]\{Fe_{1.43}Ti_{0.18}\square_{0.39}\}O_4$$

($\square$ = vacancy, [ ] = tetrahedral sites and { } = octahedral sites), with a corresponding molar mass of 208.8 g mol^{-1}. The predicted magnetization based on this formula is $\sigma \cong 68$ J T^{-1} kg^{-1}, assuming collinear spin arrangement. The large discrepancy with the experimentally determined magnetization is discussed.

Key Words—Hematite, Ilmenite, Maghemite, Magnetic Fraction, Mössbauer, Spinel.

INTRODUCTION

Tropical soils contain typically large amounts of iron oxides, particularly Hm (α-Fe_2O_3) and Mt (Fe_3O_4) or Mh (γ-Fe_2O_3). Although goethite (α-FeOOH, Gt) is a widespread mineral in soils, it appears in relatively lower proportions or is undetected by powder X-ray diffraction (XRD) in some highly weathered magnetic Oxisols forming on mafic rocks (Fontes and Weed 1991). The characterization of these minerals is important for agriculture land use as soil micro-elements' availability to plants is somehow related to their iron oxide mineralogy (Curi and Franzmeier 1987; Ferreira et al. 1993). Several recent studies have been reported on Brazilian magnetic soils. A fully oxidized titanomaghemite from a basaltic soil with a spontaneous magnetization of 36 J T^{-1} kg^{-1} was earlier characterized (Allan et al. 1989). Different Mh compositions were reported for other lithologies, e.g., the (Al, Ti)-rich Mh from a dolomitic soil (Moukarika et al. 1991) and the newly characterized Mg-rich Mh from tuffite (Fabris et al. 1995).

Basaltic bedrocks tend to produce dusky red magnetic Oxisols under tropical conditions. Although the mineralogical composition of soils derived from basalt, particularly of the clay fraction, is known from several studies (Resende 1976; Curi and Franzmeier 1987; Fontes and Weed 1991), a complete description of the nature and origin of their iron oxides appears to be not available. The present study is focused on the iron oxide mineralogy, particularly of the coarse fractions, of a Brazilian magnetic soil derived from basalt, and a more detailed description of the magnetic phases is presented.

METHODS

The soil sample was collected from the B horizon of a dusky red Oxisol developed from a tholeiitic basalt, located at geographical coordinates lat 18°36′40″S, long 49°31′45″W, in a cutting near the highway BR 154, 2 km south of Cachoeira Dourada, in the region of Triângulo Mineiro, Minas Gerais State, Brazil. The chemical composition of the parent rock and of the whole mass of the soil were reported by Pinto (1997) and Ferreira (1995) as being (in mass%), respectively: SiO_2, 46.4 (rock), 34.2 (soil); Fe_2O_3, 15.4, 26.8; Al_2O_3, 11.6, 15.9; TiO_2, 3.46, 6.89; CaO, 7.79, 0.37; MgO, 3.94, 0.91; MnO, 0.24, 0.39;

† Professor Milton Francisco de Jesus Filho died on January 2, 1996.

‡ Research Director, National Fund for Scientific Research, Belgium.

Copyright © 1998, The Clay Minerals Society

https://doi.org/10.1346/CCMN.1998.0460402 Published online by Cambridge University Press

Table 1. Chemical composition of the magnetic separates from the sand and silt fractions.

Oxide	Sand %	Silt %
FeO†	1.20	5.99
Fe_2O_3	77.97	55.59
Al_2O_3	5.50	4.05
TiO_2	8.35	30.62
CaO	0.85	0.40
MgO	0.33	0.61
MnO	0.31	0.78
BaO	0.01	0.01
Ni_2O_3	0.01	0.04
CoO	0.02	0.05
CuO	0.03	0.05
ZnO	0.04	0.17
LOI‡	5.03	4.60

† According to Goulart et al. (1994a).
‡ Loss on ignition.

P_2O_5, 0.58, Not Available (NA); Na_2O, 2.44, NA; K_2O, 1.65, NA; loss on ignition, 6.71, 12.2; total, 100.2, 97.7. The parent rock was classified according to the Jensen (1976) triangular plot, which correlates FeO + TiO_2, Al_2O_3 and MgO contents. Ilmenite (Im) (determined lattice parameter, a = 0.5082 nm and c = 1.4070 nm), augite and plagioclase (albite and/or anorthite) were the main mineralogical phases identified by XRD in the whole rock sample and Mt and a ferric Im were characterized in the magnetic extract of the tholeiitic basalt (de Jesus Filho et al. 1995). Kaolinite, Gb, Hm, Im and Mh are the main minerals in this soil.

Geologically, the sampling area is part of the Serra Geral Formation and the basalt has its origin from a Mesozoic magmatism that occurred ca. 130–150 My ago, and which covers about 1,200,000 km^2 in central and southern Brazil, northwest Uruguay, northeast Argentina and southeast Paraguay (Schobbenhaus et al. 1984).

The soil sample was first broken up by hand, left to dry in air and sieved, to obtain the fine earth (mean diameter of particles, $\phi < 2$ mm, saturation magnetization, $\sigma = 3$ J T^{-1} kg^{-1}). The sample was dispersed with a solution prepared by taking 50 mL NH_4OH 1:1 into a final volume of 500 mL, under stirring in a mixer. The suspension was then sieved to separate the sand fraction (ϕ = 0.05–2 mm; 6.7% of the soil mass). The silt (ϕ = 0.002–0.05 mm; 25.3%) and the clay ($\phi < 0.002$ mm; 68.0%) fractions were separated by centrifuging the remainder (Jackson 1969). The magnetic separates from sand and silt were obtained from a diluted slurry in water, and passed through a zigzag-shaped tube placed in a magnetic field generated by a U-shape hand magnet. Further magnetic separation was carried out by stirring the first magnetic extract in water in a beaker and collecting the magnetic particles with a small hand magnet. The proportions of magnetic separate obtained were 24 mass% (sand) and 51 mass% (silt). It was observed that the reddish magnetic separates of the clay fraction still contained a considerable amount of Hm, even after repeating the above-described procedure several times.

The chemical analysis of the magnetic separates was carried out by fusing the samples with 1:1 Na_2CO_3 + K_2CO_3 mixture in a platinum crucible and dissolving the product in diluted hydrochloric acid. The solution was then analyzed by the standard dichromatometric method (Jeffery and Hutchison 1981), with minor modifications (Neves et al. 1985) to quantify Fe, and with a Spectroflame Analytical Instruments plasma emission spectrophotometer for the other elements. The chemical composition is presented in Table 1.

The powder XRD patterns were obtained with a Diffrac 500 Siemens diffractometer, using Cu$K\alpha$ radiation.

The Mössbauer spectra were collected in a constant acceleration transmission spectrometer and a Co^{57}/Rh source, in the following experimental conditions to the sample: 1) at room temperature (RT) and 85 K; 2) at RT with an externally applied field of 0.2 T and 3) at 275 K and 4.2 K with an externally applied magnetic field of 6 T parallel to the direction of the incident γ-rays. Isomer shifts are quoted relative to metallic iron.

Magnetization measurements were made either in a conventional vibrating sample magnetometer (VSM) or with a portable soil magnetometer conceived by Coey et al. (1992).

RESULTS AND DISCUSSION

Petrographic Description

Optical microscopy analysis of the magnetic separate obtained from the sand fraction indicates light rose, isotropic euhedric-subhedric particles having white veins in 3 directions, forming triangles, which were interpreted as being Mt under an alteration process. It will be shown later that this mineral is actually Mh. Lamellae filled with a dark material identified as Im in an exsolution process were also observed.

X-Ray Diffraction

X-ray diffractograms of magnetic separates from sand and silt, as well as of the whole clay fractions, are shown in Figure 1. Reflections due to Hm, Im, Mh or Mt (see below) and Rt were identified in the magnetic separate of the sand fraction (Figure 1a). Hematite is more often an associated phase in clay (according to the definition in Guggenheim and Martin 1995), and normally it is not expected to occur as in sand-sized grains in the B horizon of the soil studied. A reasonable explanation for its presence in the sand fraction could be that this Hm acts as a coating or cementing agent in smaller individual particles, forming sand-sized aggregates. The magnetic separate of the silt fraction has additionally An and a small quantity of Ka (Figure 1b). Roughly, the silt magnetic sep-

https://doi.org/10.1346/CCMN.1998.0460402 Published online by Cambridge University Press

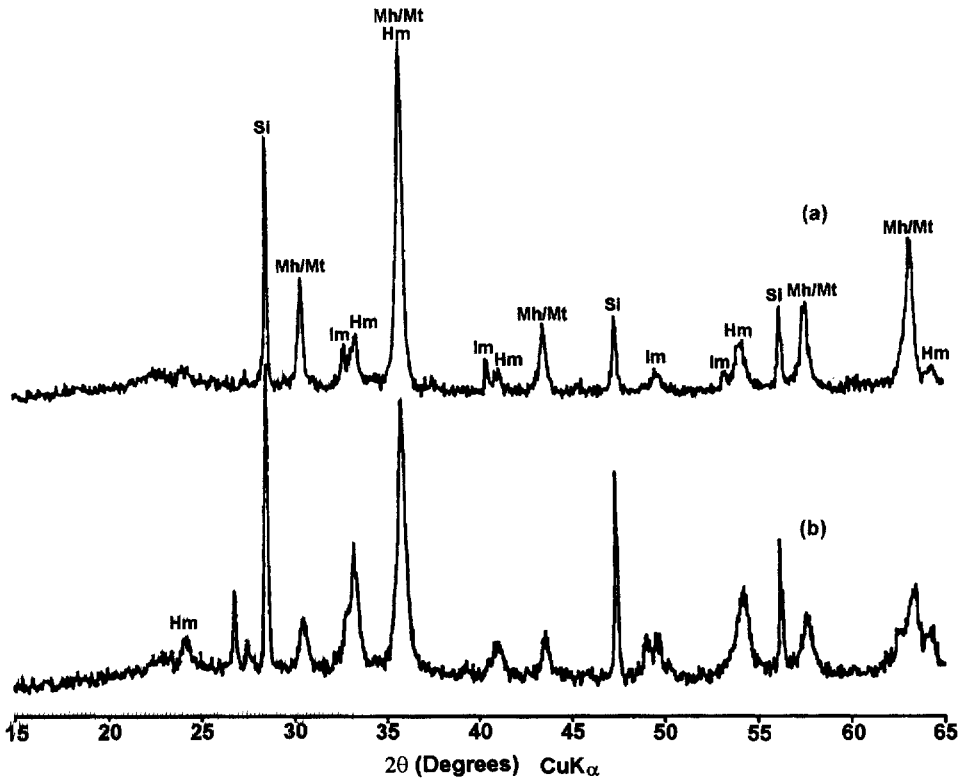


Figure 1. Powder XRD patterns (Cu$K\alpha$) of (a) sand magnetic separate, (b) silt magnetic separate and (c) whole clay. An = anatase, Gb = gibbsite, Hm = hematite, Im = ilmenite, Ka = kaolinite, Mh = maghemite, Rt = rutile, Si = silicon (internal standard).

arate and total clay fraction were found to contain qualitatively the same mineral composition as a whole, but Gb, Ka and Hm appear in higher proportion in the clay fraction (Figure 1c). Rutile was detected in all fractions.

Ditionite-citrate-bicarbonate (DCB) mixture is often used to remove noncrystalline and some crystalline iron oxides in soil samples (Mehra and Jackson 1960). Pedogenic Mh is reported to be effectively removed by DCB treatment (Fine and Singer 1989; Singer et al. 1995). In the present study, this treatment was found to be effective in preferentially removing Hm, concentrating Mh and Im, in the silt and sand fractions. This enrichment is illustrated in Figure 2 for the sand fraction.

Magnetite has been reported to be the main ferrimagnetic constituent in some tropical soils (Curi and Franzmeier 1987; Dematthê and Marconi 1991). Furthermore, it was believed to occur more often in the coarse fractions, which are more likely to contain primary minerals (Moniz 1972). However, it is difficult to identify Mt, Mh and their solid solutions in natural mixture, either by current low resolution powder XRD (Abreu and Robert 1985), the main technique used in those studies, or by optical microscopy (Anand and Glides 1984).

In the present case, the lattice parameter a_0 of the spinel structure in all samples (Table 2), deduced from the Nelson-Riley extrapolation method (Klug and Alexander 1974), using the 220, 400 and 440 reflections, are much closer to that of Mh (a_0 = 0.8339 nm, Joint Committee on Powder Diffraction Standards [JCPDS] card #4.755) than that of pure Mt (a_0 = 0.8390 nm, JCPDS card #19.629). The lower values for the cell parameters reported in Table 2 can be attributed to the effect of Al-for-Fe substitution, since replacement of Fe by titanium has no significant effect on the lattice parameter in a fully oxidized Fe-rich spinel (Readman and O'Reilly 1972).

An estimation of the amount of isomorphic Al can be done through the linear relations given by Schwertmann and Fechter (1984), Wolska and Schwertmann (1989), Gillot and Rousset (1990) or Bowen et al (1994). The results are also shown in Table 2 for the magnetic separate from the sand, before and after 4 successive treatments with DCB, and for the silt and clay fractions. The X-ray pattern of Mh in the whole clay fraction shows only 1 resolved 220 reflection that

https://doi.org/10.1346/CCMN.1998.0460402 Published online by Cambridge University Press

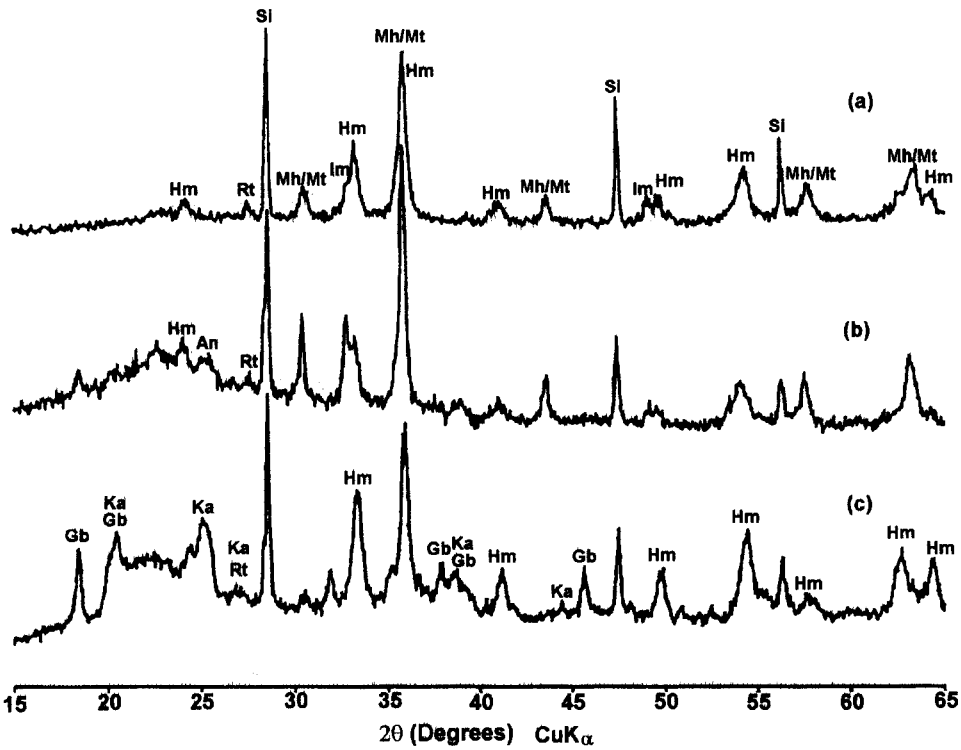


Figure 2. Powder XRD pattern (Cu$K\alpha$) of the magnetic separate from the sand fraction (a) after and (b) before 4 successive treatments with DCB. Hm = hematite, Im = ilmenite, Mh = maghemite, Si = silicon (internal standard).

does not overlap any Hm peak, but its relatively low intensity (Figure 1c) did not allow a good resolution. However, a satisfactory estimation could be done after a selective attack with 5 mol L^{-1} NaOH, to remove Gb and Ka. The lattice parameter a_0 now deduced from the better-resolved reflections of Mh, from the X-ray pattern (not shown) of the chemically treated sample, is reasonably comparable with those of the sand and silt fractions. Thus, the Mh in all 3 fractions have a similar amount of isomorphic Al substitution.

The Al substitution in the soil-Hm (Table 3) was deduced from the lattice parameter a_0, through the equation:

$$\text{Al/mol\%} = 100(32.4995 - 64.47a_0) \qquad [1]$$

taken from data of Stanjek and Schwertmann (1992), for the sand before and after (4 × DCB) 4 successive treatments with DCB, and for the silt and clay fractions. The a_0-cell parameter for Hm was determined from the 300 reflection. The Al substitution (14 mol%) of the clay Hm is in good agreement with the results obtained for other soil samples from the same region (Fontes and Weed 1991).

The mean crystallite dimension of the Hm in all fractions is 20 ± 3 nm, as deduced from the Scherrer formula (Klug and Alexander 1974), by using the values of linewidth at half height of the 110 reflection peak.

Mössbauer Spectroscopy

Mössbauer spectroscopy is, in principle, a technique capable of distinguishing among different electronic states of Fe in the oxide structure, although, in certain circumstances, some difficulties appear (da Costa, De

Table 2. Al substitution in the Mh, estimated from the lattice parameter (a_0).

Fraction	a_0/nm	Al/mol%
Sand	0.8318(5)	8
Sand (4 × DCB)	0.8319(5)	8
Silt	0.8319(5)	8
Clay	0.8326(5)	6

Table 3. Al substitution in the Hm from the magnetic separate from the sand and silt fractions, and whole-clay fraction. The a_0-cell dimension was deduced from the d(300) reflection.

Fraction	d(300)/nm	a_0/nm	Al/mol%
Sand	0.1447	0.5013(4)	18(3)
Sand (4 × DCB)	0.1446	0.5010(4)	20(3)
Silt	0.1449	0.5019(2)	14(1)
Clay	0.1449	0.5019(1)	14(1)

https://doi.org/10.1346/CCMN.1998.0460402 Published online by Cambridge University Press

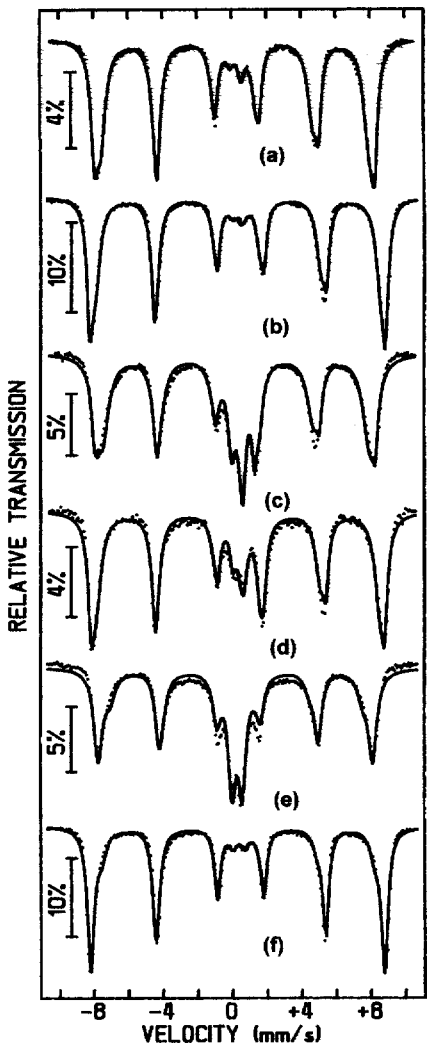


Figure 3. Mössbauer spectra of magnetic separates from the sand at (a) RT and (b) 85 K; from the silt at (c) RT and (d) 85 K; and of the whole clay fractions at (e) RT and (f) 85 K.

Grave et al. 1995). Figure 3 shows the Mössbauer spectra at RT and at 85 K of the magnetic separates obtained from sand and silt fractions and of the whole clay fraction. These spectra have been fitted as a superposition of 2 sextets, relative to Mh and Hm, together with 2 quadrupole doublets to account for ilmenite. The RT spectra of both silt and clay fractions required a third doublet that could be related to a fraction of Mh and/or Hm under superparamagnetic relaxation. The fitted spectra are not perfect, but this was expected considering the complex nature of these systems.

As mentioned above, only one sextet was included to account for Mh, but in reality there are 2 contributions, one due to Fe atoms on the tetrahedral sites and another one due to Fe atoms on the octahedral

Table 4. Mössbauer parameters at RT of the magnetic separates of the sand and silt fractions and of the whole clay.

Fraction	Subspectrum	δ/mm s^{-1}	$2\epsilon_Q$,ΔE_Q/mm s^{-1}	B_{hf}/T	A_1/%	A_2/%
Sand	Mh	0.31	0.00	48.3	65	65
	Hm	0.38	−0.18	50.4	29	30
	Im	1.03	0.68	—	2.8	1.4
		0.37	0.67	—	3.5	3.6
Silt	Mh	0.33	0.00	48.0	60	57(3)
	Hm	0.37	−0.18	50.4	16	15
	Im	1.03	0.69	—	8.6	13
		0.28	0.35	—	2.9	3.0
	Doublet	0.38	0.68	—	12	11
Clay	Mh	0.32	0.00	45.7	19	25
	Hm	0.38	−0.18	49.3	51	56(3)
	Doublet	0.38	0.60	—	29	19

Key: δ = isomer shift; ΔE_Q = quadrupole splitting; $2\epsilon_Q$ = quadrupole shift; B_{hf} = hyperfine field, A_1 = relative area of the subspectrum, without externally applied magnetic field, A_2 = relative area under an external field of 0.2 T, Mh = maghemite, Hm = hematite, Im = ilmenite.

ones. Another shortcoming of this fitting procedure is that most probably all components show a distribution of hyperfine fields and quadrupole splittings due to the isomorphic substitution by Al and Ti. In spite of that, some semiquantitative conclusions can be drawn from the results listed in Tables 4 and 5. Some room-temperature Mössbauer parameters for bulk Mt, Hm, Mh and Im were compiled by Murad and Johnston (1987), Bowen et al. (1993) and Murad (1996), and are presented in Table 6 for comparative purpose.

Based on the values of the relative subspectral areas, it is seen that Mh is indeed the major component in the sand and silt fractions, whereas Hm dominates in the clay fraction. The quadrupole shift of the latter remains unchanged on going from RT to 85 K, indicating that this Hm is in the weakly ferromagnetic state, i.e., there was no Morin transition. The more intense absorption in the central part of the spectrum

Table 5. Mössbauer parameters at 85 K of the magnetic separates of the sand and silt fractions and of the whole clay.

Fraction	Subspectrum	δ/mm s^{-1}	$2\epsilon_Q$,ΔE_Q/mm s^{-1}	B_{hf}/T	A/%
Sand	Mh	0.43	0.00	51.4	60
	Hm	0.50	−0.18	53.2	34
	Im	1.14	1.16	—	3
		0.41	0.68	—	3
Silt	Mh	0.42	0.00	51.0	57
	Hm	0.51	−0.18	52.8	26
	Im	1.18	1.16	—	11
		0.45	0.68	—	6
Clay	Mh	0.43	0.00	49.0	18
	Hm	0.48	−0.18	52.7	77
		0.48	0.68	—	5

Key: δ = isomer shift, ΔE_Q = quadrupole splitting; $2\epsilon_Q$ = quadrupole shift, B_{hf} = hyperfine field, A = relative area.

https://doi.org/10.1346/CCMN.1998.0460402 Published online by Cambridge University Press

Table 6. Room temperature Mössbauer parameters for bulk Mt, Hm, Mh and Im (adapted Murad and Johnston (1987), Bowen et al. (1993) and Murad (1996)).

Mineral	Formula	δ/mm s^{-1}	$2\epsilon_Q\Delta E_Q$/ mm s^{-1}	B_{hf}/T
Mt	Fe_3O_3	0.26	≤|0.02|	49.2
		0.67	≤|0.02|	46.1
Hm	αFe_2O_3	0.37	−0.20	51.8
Mh	γFe_2O_3	0.23	≤|0.02|	50.0
		0.35	≤|0.02|	50.0
Im	$FeTiO_3$	1.07	0.68	—

at 85 K of the silt is attributed to the ferric Im $Fe_{1.15}Ti_{0.85}O_3$, described by Goulart et al. (1994a).

The Al substitution in the clay Hm, estimated using the equation:

$$B_{eff}\,(RT) = 51.7 - 7.6\ Al - 32/MCD \qquad [2]$$

(Murad and Schwertmann 1986) and considering MCD = 20 nm, is 11 mol%. The corrections for small-particle effects can be neglected at 85 K, and the equation:

$$B_{eff} = 532 - 0.39x \qquad [3]$$

(De Grave et al. 1982) gives x = 13 mol%. Both results are in reasonable agreement with that estimated from XRD, namely, x = 14 mol%. Similar calculation could not be done for the silt and sand Hm due to its small contribution to the overall spectral area.

As for the Mh component, no conclusion can be drawn with respect to the isomorphic substitution. The hyperfine fields listed in Tables 4 and 5 must be considered as a rough estimation, since they only represent the average between the A- and B-site contributions. Also, the presence of Hm in large quantities seriously influences the fitted parameters. In all likelihood, these measurements clearly show that any Mt, if present in these samples, represents only a minor fraction and that Mh is by far the main ferrimagnetic component.

It has been shown that an external magnetic field of 0.2 T at RT would be sufficient to improve the semi-quantitative estimation of the relative Mössbauer absorption areas of the 2 subspectra in synthetic mixtures of Hm-Mh (Goulart et al. 1994b). However, the results presented in Table 4 indicate that the Mössbauer analysis of these natural iron oxide phases is only moderately improved under such an externally moderate applied magnetic field (Figure 4).

The influence of the 4 × DCB treatment on the Mössbauer spectra in an external field of 0.2 T of the sand and silt fractions are shown in Figure 4. The residual intensities of lines 2 (rightside line relative to the leftmost line 1) and 5 (leftside line relative to the rightmost line 6) are mainly due to Hm, as these absorptions would tend to almost vanish in the case of pure Mh with particle sizes of the order of those in the present study. The DCB-treated samples show much lower intensities of lines 2 and 5 as compared to the untreated samples, indicating a decrease of the Hm content, which is consistent with the XRD results. As a general trend, an increase of the Mh/Hm ratio in both sand and silt fractions is observed after DCB treatment, inferring that this chemical treatment is preferentially removing Hm. A similar result was earlier reported by Taylor and Schwertmann (1974). This preferential removal of Hm could suggest that treating the samples a few more times with DCB would lead to a higher enrichment in the ferrimagnetic component, but it was observed that some Mh is actually attacked by the DCB. This is clearly seen from the saturation magnetization values for the sand-magnetic

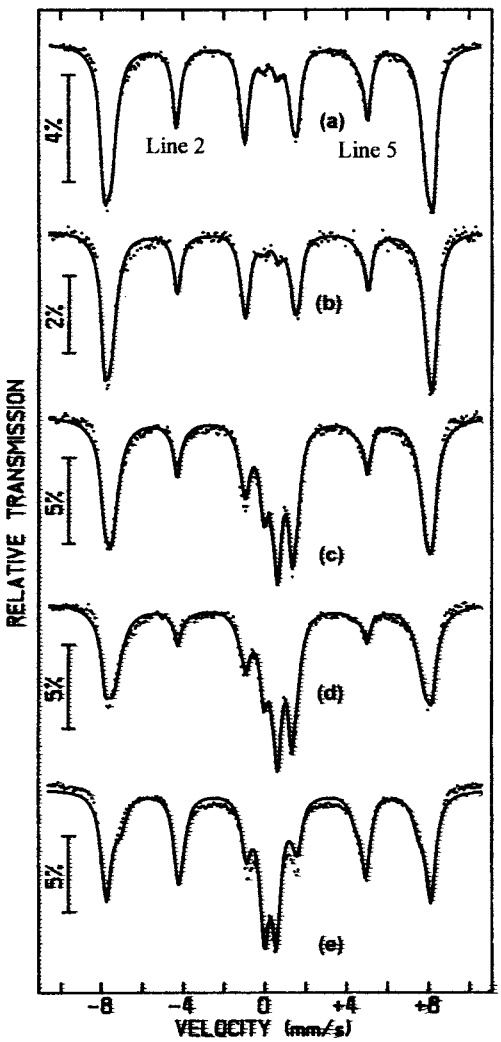


Figure 4. Mössbauer spectra of the sand fraction magnetic separate (a) before and (b) after 4 successive treatments with DCB (4 × DCB), of the silt fraction (c) before and (d) after 4 × DCB and (e) of the whole clay fraction, all under an externally applied magnetic field of 0.2 T.

https://doi.org/10.1346/CCMN.1998.0460402 Published online by Cambridge University Press

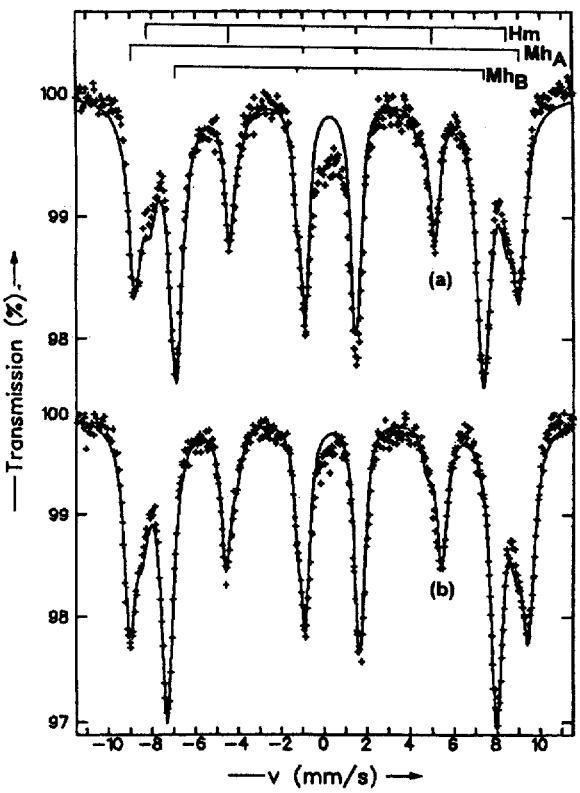


Figure 5. Mössbauer spectra of the sand fraction magnetic separate at (a) 273 K and (b) 4.2 K under an externally applied magnetic field of 6 T.

separate before (35 J T^{-1} kg^{-1}) and after DCB treatment (33 J T^{-1} kg^{-1}), and for the corresponding silt-magnetic separate values (16 J T^{-1} kg^{-1} and 12 J T^{-1} kg^{-1}, respectively).

In a stronger external field of 6 T, the Mh spectrum splits into 2 subspectra relative to the tetrahedral and octahedral sites, because the A-site hyperfine field adds to and the B-site subtracts from the applied external field. At 4.2 K, no important superparamagnetic relaxation effect is observed, and hence the assignment of the hyperfine parameters for Mh and Hm can be substantially improved. Two example spectra at 273 K and 4.2 K are displayed in Figure 5 for the sand-fraction's magnetic separate. The presence of 3 magnetic components is evident, plus a central absorption, which is more pronounced in the 273-K spectrum. No attempts were made to fit the central absorption in the 273-K spectrum because it lacks any fine structure. Probably this component is in fact a triplet since Im is paramagnetic at that temperature. In the 4.2 K, this central contribution almost disappeared, but it was not found possible to include another sextet to account for the magnetic splitting of the Im.

As for the 3 main sextets, the following restrictions were used in the fitting procedure: pure Lorentzian-shaped sextets with the isomer shift for Hm coupled to that of the B-site of Mh; line-area ratios as 3:x:1 for Mh and 3:3.6:1 for Hm (De Grave et al. 1992); quadrupole shifts $\epsilon_Q = 0$ for both sites of Mh. Some numerical parameters derived from this fitting routine are given in Table 7. Taking an average value of the relative spectral area for Im from all spectra measured without the strong field, the ratio of the relative areas Mh : Hm : Im is found to be 71:26:3. This ratio is in disaccord with those derived from the zero-field measurements (RT and 85 K), showing that the latter measurements are not adequate to fully characterize this kind of material. Furthermore, even the hyperfine fields are affected by a large uncertainty due to the strong overlap of all 3 subspectra. Thus, any attempt to correlate the low values of these hyperfine fields with isomorphic substitution would only have a qualitative meaning. A difference of about 0.12 mm s^{-1} was found both at 4.2 K and 275 K, in agreement with the values reported by da Costa, De Grave, Vandenberghe et al. (1994) and da Costa, De Grave, Bryan and Bowen (1994).

Table 7. Mössbauer parameters of the magnetic separate of the sand fraction under an external field of 6.0 T.

	Mh			Hm			
T(K)	δ/mm s^{-1}	B_{hf}/T	A/%	δ/mm s^{-1}	$2\epsilon_Q$/ mm s^{-1}	B_{hf}/T	A/%
273	0.21	49.2	24	0.33	−0.18	51.2	23
	0.33	50.2	43				
4.2	0.31	51.2	26	0.43	−0.20	53.7	26
	0.44	53.3	45				

Key: δ = isomer shift; $2\epsilon_Q$ = quadrupole shift; B_{hf} = hyperfine field, A = relative area.

Another important observation is that the high intensities of the middle lines of the hematite component (3:3:4:1), together with a negative value for the quadrupole shift, indicate that this oxide is in the weakly ferromagnetic state, even at 4.2 K (De Grave et al. 1992; Bowen and De Grave 1995). The suppression of the Morin transition is presumably due to the presence of Al and/or Ti in the Hm structure, to which this transition is extremely sensitive. A 1% Ti-substitution is sufficient to eliminate the antiferromagnetic state (Ericsson et al. 1986), while approximately 9% of Al is required to create the same effect (Coey 1988).

Based on the Al content in Hm and Mh as deduced from XRD, and on the proportions of these 2 phases derived from the in-field Mössbauer spectra, the overall allocation gives about 5.3 mass% Al_2O_3 in the sand fraction. This result is in good agreement with the total 5.50 mass% Al_2O_3 found in the chemical analysis (Table 1). Diagenetic Hm is likely to retain only trivalent structural cations in its structure. Di and tetravalent cations are expelled from the lattice on passing from Mh to Hm (Sidhu et al. 1980), an expected process in

https://doi.org/10.1346/CCMN.1998.0460402 Published online by Cambridge University Press

soil-mineral genesis. Thus, discarding any eventual Ti in the Hm, the Mh would contain 7 mass% TiO_2, taking into account that 1.3 mass% TiO_2 must be allocated to the ferric Im. The combined effect of both Al and Ti can explain the absence of the Morin transition down to 4.2 K.

The question now is how to distribute Fe, Al, Ti and vacancies between the 2 sublattices of Mh. The A- to B-site area ratio as derived from the 6 T Mössbauer spectra is 37:63, but this ratio may be underestimated as Hm lines overlap with those of A-site. Several recent studies have shown that Al has no site preference, its location being dependent on the synthesis procedure and on its concentration. Actually, there are reports in which all Al are located exclusively on the A sites (da Costa, De Grave, Bryan and Bowen 1994), on the B sites (de Jesus Filho et al. 1992; Allan et al. 1989; Bowen et al. 1994) or on both sites (Wolska and Schwertmann 1989; da Costa, Laurent et al. 1995). In the present case, from Fe distribution, it may be occupying only A-sites. On the other hand, it is known that Ti has a strong B-site preference (Waychunas 1991). As for the vacancies, it is usually assumed that in relatively well-crystallized Mh, which is the case for the present samples, they are located on B-sites (Lindsley 1976; Bowen et al. 1994). The suggested stoichiometric spinel formula, based upon the deduced elemental composition of Al_2O_3 (8%) and TiO_2 (7%) and Fe_2O_3 (85%, the complement to 100%) for the sand-Mh, and assigning Al on A and Ti and vacancies on the B site is:

$$[Fe_{0.92}Al_{0.08}]\{Fe_{1.43}Ti_{0.18}\square_{0.39}\}O_4$$

($\square$ = vacancy, [ ] = tetrahedral sites and { } = octahedral sites), with a corresponding molar mass of 208.8 g mol^{-1}.

The saturation magnetization of the sand magnetic separate is 35 J T^{-1} kg^{-1}, which gives around 49 J T^{-1} kg^{-1} for the soil Mh. The above formula corresponds to a magnetization of 68 J T^{-1} kg^{-1}, assuming a moment of 5 μ_B on the Fe ions and a collinear ferrimagnetic spin structure. Several effects can contribute to the discrepancy between the determined magnetization (49 J T^{-1} kg^{-1}) relative to the predicted value from the allocated formula, as for example, small-particle sizes (Mørup and Topsøe 1976), inter- and intra-particle interactions (Mørup and Tronc 1994), surface effects (Boudeulle et al. 1983) and spin reduction due to covalence (Greaves 1983). Spin canting has an important influence on the magnetization of randomly substituted spinel ferrites (Coey 1987). In addition, the site occupancy and the amount of substitution are not known with great precision, making it extremely difficult to derive the true composition. Much stronger external fields, of the order of 15 T, would be very useful in order to completely separate the A- and B-site contributions of Mh from that of Hm.

CONCLUSIONS

The present study on the mineralogy of a Brazilian dusky red magnetic Oxisol was focused on the characterization of the Fe-bearing minerals of the magnetic separate from the sand and silt fractions. Hematite is mainly present in the whole clay fraction, together with Gb, Ka, Rt (and probably An) and Mh. Maghemite, which contributes by about 6% to the whole soil mass, is the dominant mineral in the magnetic separate (in sand, about 65% of the relative Mössbauer spectral area; silt, 60%). Hematite (sand, 30%; silt, 15%) and Im (sand, 5%; silt, 16%) are also significantly present in the silt fraction. Accessory minerals are Rt and An. No Mt was detected in the magnetic extract of any soil fraction. Sand- and silt-Mh have similar cell parameters (a_0 = 0.8319 ± 0.0005 nm) and saturation magnetizations of 49 J T^{-1} kg^{-1}. Hematite, an associated phase in clay, was also detected in the sand-magnetic separate. The Al content in Hm varies from 14 mol% (clay- and silt-Hm) to 20 mol% (sand). The proposed cation distribution among the spinel sites of the soil-Mh leads to an expected magnetization $\sigma \cong 82$ J T^{-1} kg^{-1}, assuming collinear spin arrangement.

ACKNOWLEDGMENTS

This paper is dedicated to the memory of Professor M. F. de Jesus Filho. The authors are indebted to D. Prudente Santana (CNPMS/EMBRAPA) and N. Curi (ESAL) for their help in selecting and collecting samples and to G. Pereira Santana (postgraduate student at Department of Chemistry, UFMG, Brazil) for his technical support on the Mössbauer measurements. We are also indebted to M. B. Harmendani Vieira, Technology Centre, Vale do Rio Doce Co., Santa Luzia, MG, Brazil, for the optical microscope analysis work financially supported by CNPq, FINEP and Fapemig (Brazil), ISC-European Commission (CT90-0856) and the Fund for Joint Basic Research, Belgium (G 2014.93).

REFERENCES

Abreu MM, Robert MN. 1985. Characterization of maghemite in B horizons of three soils from Southern Portugal. Geoderma 56:97–108.

Allan JEM, Coey JMD, Sanders IS, Schwertmann U, Friedrich G, Wichowski A. 1989. An occurrence of a fully oxidized natural titanomaghemite in basalt. Mineral Mag 53: 299–304.

Anand RR, Glides RJ. 1984. Mineralogical and chemical properties of weathered magnetite grains from lateritic saprolite. J Soil Sci 35:559–567.

Boudeulle M, Batis-Landoulsi H, Leclerq CH, Vergnon P. 1983. Structure of γFe_2O_3 microcrystals: Vacancy distribution and structure. J Solid State Chem 48:21–32.

Bowen LH, De Grave E. 1995. Mössbauer spectra in external field of highly substituted aluminous hematites. J Magn Magn Mater 139:6–10.

Bowen LH, De Grave E, Bryan AM. 1994. Mössbauer studies in external field of well crystallized Al-maghemites made from hematite. Hyperfine Interact 94:1977–1982.

Bowen LH, De Grave E, Vandenberghe RE. 1993. Mössbauer effect studies of magnetic soils and sediments. In: Long GJ, Grandjean F, editors. Mössbauer spectroscopy applied to magnetism and material science. New York: Plenum Pr. p 115–159.

https://doi.org/10.1346/CCMN.1998.0460402 Published online by Cambridge University Press

Coey JMD. 1987. Noncollinear spin structures. Can J Phys 65:1210–1232.

Coey JMD. 1988. Magnetic properties of iron in soil iron oxides and clay minerals. In: Stucki JW, Goodman BA, Schwertmann U, editors. Iron in soil and clay minerals. Dordrecht: Reidel. p 397–465.

Coey JMD, Cugat O, McCauley J, Fabris JD. 1992. A portable soil magnetometer. Revista de Física Aplicada e Instrumentação 7:25–30.

da Costa GM, De Grave E, de Bakker PMA, Vandenberghe RE. 1995. Influence of nonstoichiometry and the presence of maghemite on the Mössbauer spectrum of magnetite. Clays Clay Miner 43:656–668.

da Costa GM, De Grave E, Bryan AM, Bowen LH. 1994. Mössbauer studies of nano-sized aluminium-substituted maghemites. Hyperfine Interact 94:1983–1987.

da Costa GM, De Grave E, Vandenberghe RE, Bowen LH, de Bakker PMA. 1994. The center shift in the Mössbauer spectra of maghemite and aluminium maghemites. Clays Clay Miner 42:628–633.

da Costa GM, Laurent CH, De Grave E, Vandenberghe RE. 1995. A comprehensive Mössbauer study of highly-substituted aluminum maghemites. Mineral spectroscopy: A tribute to R. G. Burns. Dyar MD, McCammon C, Schaefer MW, editors. Geochem Soc Spec Publ 5:93–104.

Curi N, Franzmeier DP. 1987. Effect of parent rocks on chemical and mineralogical properties of some oxisols in Brazil. Soil Sci Soc Am J 51:153–158.

De Grave E, de Bakker PMA, Bowen LH, Vandenberghe RE. 1992. Effect of crystallinity and Al substitution on the applied-field Mössbauer spectra of iron oxide and oxyhydroxides. Z Pflanzenernähr Bodenk 155:467–472.

De Grave E, Bowen LH, Weed SB. 1982. Mössbauer study of aluminum-substituted hematites. J Magn Magn Mater 27:98–108.

Demattê JLI, Marconi A. 1991. A drenagem na mineralogia de solos desenvolvidos de diabásio em Piracicaba. R Bras Ci Solo 15:1–8.

Ericsson T, Krisnhamarthy A, Srivastava, BK. 1986. Morin transition in Ti-substituted hematite: A Mössbauer study. Phys Scripta 33:88–90.

Fabris JD, Coey JMD, Qinian Qi, Mussel W da N. 1995. Characterization of Mg-rich maghemite. Am Mineral 80: 664–669.

Ferreira BA. 1995. Caracterização fisico-química de minerais ferruginosos de um pedossistema desenvolvido de basalto [MSc thesis]. Belo Horizonte, Brazil: Federal Univ of Minas Gerais. 99 p.

Ferreira SAD, Santana DP, Fabris JD, Curi N, Nunes Filho E, Coey JMD. 1993. Relações entre magnetização, elementos traços e litologia de duas sequências de solos do Estado de Minas Gerais. Rev Bras Ci Solo 18:167–174.

Fine P, Singer MJ. 1989. Contribution of ferrimagnetic minerals to oxalate- and dithionite-extractable iron. Soil Sci Soc Am J 53:191–196.

Fontes MPF, Weed SB. 1991. Iron oxides in selected Brazilian Oxisols. I: Mineralogy. Soil Sci Soc Am J 55:1143–1149.

Gillot B, Rousset A. 1990. On the limit of aluminum substitution in Fe_3O_4 and γFe_2O_3. Phys Status Solidi (a) 118:K5–K8.

Goulart AT, de Jesus Filho MF, Fabris JD, Coey JMD. 1994a. Characterization of a soil ilmenite developed from basalt. Hyperfine Interact 91:771–775.

Goulart AT, de Jesus Filho MF, Fabris JD, Coey JMD. 1994b. Quantitative Mössbauer analysis of maghemite-hematite mixtures in external applied field. Hyperfine Interact 83: 451–455.

Greaves C. 1983. A powder neutron diffraction investigation of vacancy ordering and covalence in γFe_2O_3. J Solid State Chem 49:325–333.

Guggenheim S, Martin RT. 1995. Definition of clay and clay mineral: Joint report of the AIPEA nomenclature and CMS nomenclature committees. Clays Clay Miner 43:255–256.

Jackson ML. 1969. Soil chemical analysis—Advanced course. Madison, WI: ML Jackson. 894 p.

Jeffery PG, Hutchison D. 1981. Chemical methods of rock analysis. Oxford: Pergamon Pr. 379 p.

Jensen LS. 1976. A new cation plot for classifying subalkalic volcanic rocks. Ontario: Department of Mines, Misc Paper 66.

de Jesus Filho MF, Fabris JD, Goulart AT, Coey JMD, Ferreira BA, Pinto MCF. 1995. Ilmenite and magnetite of a tholeiitic basalt. Clays Clay Miner 43:641–642.

de Jesus Filho MF, Mussel W da N, Qinian Qi, Coey JMD. 1992. Magnetic properties of aluminium-doped γFe_2O_3. In: Yamaguchi T, Abe M, editors. Proc 6th Int Conf on Ferrites (ICF 6); The Japan Society of Powder and Powder Metallurgy; Tokyo, Japan. p 126–128.

Klug HP, Alexander LE. 1974. X-ray diffraction procedures for polycrystalline and amorphous materials. New York: J. Wiley. 966 p.

Lindsley DH. 1976. The crystal chemistry and structure of oxide minerals as exemplified by the Fe-Ti oxides. Rev Mineral 3:L1–L60.

Mehra OP, Jackson ML. 1960. Iron oxide removal from soils and clay a dithionite-citrate system buffered with sodium bicarbonate. Clays Clay Miner 7:317–327.

Moniz AA. 1972. Elementos de pedologia. São Paulo: Editora Polígono. 459 p.

Mørup S, Topsøe H. 1976. Mössbauer studies of thermal excitations in magnetically ordered microcrystals. Appl Phys 11:63–66.

Mørup S, Tronc E. 1994. Superparamagnetic relaxation of weakly interacting particles. Phys Rev Lett 72:3278–3281.

Moukarika A, O'Brien P, Coey JMD, Resende M. 1991. Development of magnetic soil from ferroan dolomite. Geophys Res Lett 18:2043–2045.

Murad E. 1996. Magnetic properties of microcrystalline iron(III) oxides and related materials as reflected in their Mössbauer spectra. Phys Chem Minerals 23:248–262.

Murad E, Johnston JH. 1987. Iron oxides and oxyhydroxides. In: Long GJ, editor. Mössbauer spectroscopy applied to inorganic chemistry, vol. 2. New York: Plenum Pr. p 507–582.

Murad E, Schwertmann U. 1986. Influence of Al substitution and crystal size on the room temperature Mössbauer spectrum of hematite. Clays Clay Miner 34:1–6.

Neves AA, Goulart AT, Garotti FV. 1985. Caracterização da interferência da platina, na análise de ferro em amostras naturais. Química Nova 8:152–154.

Pinto MCF. 1997. Caracterização e establidade ligogenética da magnetica de rochas máficas [MSc thesis]. Belo Horizonte, Brazil: Federal Univ of Minas Gerais. 75 p (in Portuguese).

Readman PW, O'Reilly W. 1972. Magnetic properties of oxidized (cation-deficient) titanomagnetites $(FeTi_{-})_3O_4$. J Geomagn Geoelect 24:69–90.

Resende M. 1976. Mineralogy, chemistry, morphology and geomorphology of some soils of the central plateau of Brazil [Ph.D. thesis]. Purdue Univ. Diss Abstracts 37:4803.

Schobbenhaus C, Campos D de A, Derze GR, Asmus HE. 1984. Formação Mata da Corda (kmc). In: Ministério das Minas e Energia/DNPM. Geologia do Brasil: Texto explicativo do mapa geológico do Brasil e da área oceânica adjacente incluindo depósitos minerais. Brasília. p 348.

https://doi.org/10.1346/CCMN.1998.0460402 Published online by Cambridge University Press

Schwertmann U, Fechter H. 1984. The influence of aluminum on iron oxides: XI. Aluminum-substituted in soils and its formation. Soil Sci Soc Am J 48:1462–1463.

Sidhu PS, Gilkes RJ, Posner AM. 1980. The behavior of Co, Ni, Zn, Cu, Mn, and Cr in magnetite during alteration to maghemite and hematite. Soil Sci Soc Am J 44:135–138.

Singer MJ, Bowen LH, Verosub KL, Fine P, TenPas J. 1995. Mossbauer spectroscopic evidence for citrate-bicarbonate-dithionite extraction of maghemite from soils. Clays Clay Miner 43:1–7.

Stanjek, H, Schwertmann U. 1992. The influence of aluminum on iron oxides. Part XVI: Hydroxyl and aluminum substitution in synthetic hematites. Clays Clay Miner 40: 347–354.

Taylor RM, Schwertmann U. 1974. Maghemite in soils and its origin. 1. Properties and observation on soil maghemites. Clays Clay Miner 10:289–298.

Waychunas GA. 1991. Cystal chemistry of oxides and oxhydroxides. In: Lindslay GH, editor. Rev Mineral 25, Oxide minerals: Petrologic and magnetic significance. Mineral Soc Am. p 12–68.

Wolska E, Schwertmann U. 1989. The vacancy ordering and distribution of aluminum ions in $(Fe,Al)_2O_3$. Solid State Ionics 32/33:214–218.

(Received 28 June 1996; accepted 13 August 1997; Ms. 2786)

https://doi.org/10.1346/CCMN.1998.0460402 Published online by Cambridge University Press